Electronic structure of the single-domain Si(111)-(3×1)-Li surface

C. Bromberger,[1,*] J. N. Crain,[2] K. N. Altmann,[2] J. J. Paggel,[3] F. J. Himpsel,[2] and D. Fick[1,2]
[1]*Philipps-Universität, Fachbereich Physik and Zentrum für Materialwissenschaften, D-35032 Marburg, Germany*
[2]*Department of Physics, University of Wisconsin–Madison, Madison, Wisconsin 53706, USA*
[3]*Freie Universität Berlin, Institut für Experimentalphysik I, D-14195 Berlin, Germany*
(Received 2 December 2002; revised manuscript received 8 May 2003; published 28 August 2003)

The band structure of the single-domain Si(111)-(3×1)-Li surface is investigated by angular resolved photoelectron spectroscopy (ARPES) with synchrotron radiation. Vicinal surfaces are used as templates for obtaining a single-domain (3×1) reconstruction. The surface band structure consists of a single, well-pronounced state at about 0.9 eV below the valence band maximum. Its dispersion matches local density calculations for the honeycomb-chain-channel (HCC) structure, but the calculated energy is 0.31 eV too high. This shift is reminiscent of localized surface states on other silicon surfaces, such as Si(111)-H.

DOI: 10.1103/PhysRevB.68.075320 PACS number(s): 73.20.At, 72.80.Cw, 79.60.Bm

I. INTRODUCTION

Low-dimensional systems have attracted a great deal of interest due to their unusual electronic properties. In recent years, a new type of one-dimensional system has been created by self-assembly of atomic chains at stepped surfaces (for an overview see Ref. 1). These are, in principle, ideal systems to observe the change from two-dimensional to one-dimensional character by changing the step spacing. One-dimensional systems are predicted to display strange features sometimes due to the strong electron-electron correlations that are imposed on electrons confined to a single direction in space.

Si(111) and its vicinal surfaces, in particular, have shown a wealth of chain structures after depositing metal atoms in the submonolayer regime. Metallic chains have been found with In (Ref. 2) and with Au on a variety of vicinal surfaces.[3–10] Semiconducting (3×1) structures are formed by alkali metals, alkaline earths, and by Ag.[11–24]

Our focus lies on the fairly large group of metal-driven (3×1) reconstructions that spontaneously break the threefold symmetry of the flat Si(111) surface. They can be formed by a rather simple procedure (see Ref. 13, and references therein). In addition to their quasi-one-dimensional structure they exhibit quite unusual chemical and electronic properties for an alkali-covered surface, such as low oxygen uptake[25] and a large surface band gap of about 1 eV.[26]

Since its first observation[11,12] the (3×1) reconstruction of the Si(111) surface has generated widespread interest. Despite some uncertainties about the details of the atomic arrangement there is a consensus that this reconstruction is driven by the metal adsorbate and that it occurs for monovalent adsorbates at a metal coverage of 1/3 of a monolayer, measured in units of one Si(111) layer (see Refs. 13,15,18,20,21, and references therein). In all the structural models[15–19,27] the metal atoms form one chain per unit cell, which are separated by Si chains. Among the proposed structural models, the recent ''560560'' model[16,17] and the similar honeycomb-chain-channel (HCC) model[18] have the lowest total energies and explain most of the structural features seen in STM and diffraction experiments. These two models contain almost the same arrangement of the surface atoms (see Fig. 1 in Ref. 16 for the ''560560'' model and Fig. 1 in Ref. 18 for the HCC model). There are four nonequivalent Si surface atoms which form a planar honeycomb chain parallel to the surface while the metal atoms form a row in between these chains. For the ''560560'' model this configuration follows from a rehybridization of a Si atom from a sp^3 to a sp^2 configuration which just leads to three planar bonds with angles of 120° each in between them. In the HCC model the planar configuration is thought to be a consequence of a Si double bond as the four top Si atoms have almost the same configuration as the planar disilene (Si_2H_4). The calculated electron density plots[18] support this explanation.

From energy considerations it seems obvious that the alkali metal atoms act as electron donors, saturating the unpaired Si dangling bond in the (3×1) reconstruction. This aside, very little is known about the role of the metal atom in the reconstruction itself. Recent NMR experiments[22,28] contributed new information about the local geometry and the electronic structure of the Li site. A large, positive electric field gradient at the adsorbed Li nucleus places the Li site inside surrounding Si atoms and not above the surface, in accordance with the ''560560'' and HCC models. The question of a completely ionized Li atom which is an essential component of the HCC-model[18] will be accessible to an experimental test through nuclear spin relaxation experiments (T_1 times).[29,30] If theoretical predictions of a completely ionized Li adsorbate in the (3×1) reconstruction are true,[18] the relaxation rate $1/T_1$ should vanish (no *s*-electron density at the nucleus).

Even though the (3×1) reconstruction can be obtained by adsorption of various metal atoms, such as Li, Na, K, Ag, Mg, Ca, or Ba, the Li-induced reconstruction is of special importance because of the simple electronic structure of Li and its accessibility to NMR measurements. The favored models (HCC and ''560560'') have five Si surface orbitals per unit cell and thus five surface states. There are altogether six electrons available to fill these states, five from the Si atoms and one from the Li atom. Since the surface is semiconducting we expect three filled surface states and two empty ones. There is no calculated band structure for the ''560560'' model. The calculated band structure of the HCC model,[18] however, confirms this reasoning with three occu-

pied surface state bands S_1^+, S_2^+, and S_2^-. The symmetry of the S_2^- state prevents it to be observed in our photoemission geometry (p-polarized light with the plane of incidence including the chain direction). Therefore, we expect to see two occupied surface states. However, only one surface state was observed in a previous experiment using the same geometry but samples with three domains.[31] Thereby, emission from three regions of the surface Brillouin zone becomes mixed and blurs the features in k space.

In order to clarify the $E(k)$ band dispersion further we have set out to map the bands of a single domain. In addition, we use improved experimental equipment that has become available in the meantime, such as energy plus angle multidetection. Using synchrotron radiation the photon energy is tuned to the optimum cross section for detecting surface states on Si(111), which is near 34 eV (Refs. 5,8,32,33, and references therein).

The easiest way to produce a three domain Li-induced (3×1)-reconstructed Si(111) surface is Li adsorption and subsequent thermal desorption of the excess amount to receive the (3×1) structure.[13] This preparation relies entirely on thermal programmed desorption (TPD) spectroscopy and produces the desired structure reproducibly with minimum effort. Since our arguments above rely to a large extent on electron counting, it is important to know the absolute coverage of the metal semiconductor interface.[34] Both topics, preparation and coverage determination, have been extensively described in separate papers.[13,35]

A single-domain (3×1) reconstruction is obtained from Si(111) surfaces slightly miscut towards the $[\bar{1}\bar{1}2]$ azimuthal direction. The resulting steps are used as template to orient the Li chains parallel to the step edges.[1,7,8,36,37] With this method we are able to acquire spectra for well-defined momenta both parallel and perpendicular to the chains.

II. EXPERIMENT

The ARPES spectra were taken at a substrate temperature between 200 and 300 K with a hemispherical SCIENTA photoelectron spectrometer (SES 200) equipped with energy and angle multidetection. It was coupled to a 4 m normal incidence monochromator at the Synchrotron Radiation Center (SRC) in Madison. Connected to the analyzer chamber was a preparation chamber where low-energy electron diffraction (LEED), a Li getter source (SAES Getters), and sample heating was available. The base pressure in the preparation chamber was at 1.5×10^{-10} mbar and the one in the analyzer chamber was believed to be in the same range. There was no ion gauge installed near the sample, since firstly the free ions from it lead to an enhanced deposition of rest gas atoms and or molecules on the sample surface and secondly the electrostatic fields of the ion gauge may distort the static electric spectrometer fields. From the readings of the other ion gauges in the chamber and from the fading rate of the (3×1) surface state we believed, however, that the pressure at the sample has to be around a few 10^{-10} mbar.

The samples were 4×18 mm^2 large slices of 0.5 mm thick vicinal Si(111) wafers. The data shown are for a miscut of 2° in the $[\bar{1}\bar{1}2]$ direction. The samples were clamped at one side between Ta plates and on the other side between sapphire plates with a Ta contact sheet to allow resistive heating. The heating current was passed parallel to the steps in order to avoid electromigration effects and step bunching.[38] The temperature was measured with an optical infrared pyrometer. Sample and holder were outgassed at 970 K for at least half an hour. A clean surface was obtained by flashing the samples several times up to 1520 K for a few seconds where the native oxide evaporates and the residual surface carbon diffuses into the bulk. After the last flash, the samples were postannealed at 1100 K for about 3 min to obtain a (7×7) surface with straight steps.[37] We started the preparation of the Li induced (3×1) structure by depositing about three monolayers of Li at room temperature, measured with a quartz crystal monitor in front of the sample. A thoroughly outgassed Li getter source was used. As the (3×1)-Li reconstruction forms at a coverage of 1/3 of a monolayer, we flashed the sample afterwards to 860 K to desorb the surplus Li.[13,35]

We found that it is possible to produce Li-induced single-domain (3×1) reconstructions using vicinal Si(111) samples,[39] while, for example, on the Na induced one even on vicinal surfaces all domains are evenly distributed with a slight preference for the $[1\bar{1}0]$ direction.[14] In order to obtain a perfect single domain (3×1) reconstruction we tested samples with various miscuts. For a sample miscut between 0° and 0.5° this procedure led always to a three domain reconstructed surface. However, already at a sample miscut of 1° the surface was predominantly single domain. The sample eventually used for the photoemission experiments (n type, arsenic doped, 0.005 Ω cm) had a miscut of 2° towards the $[2\bar{1}\bar{1}]$ direction. With this sample the preparation procedure led in its center area to a perfect single domain (3×1) surface with no other domains visible by LEED [Fig. 1(a)]. In Fig. 1(b) the corresponding surface Brillouin zones of the Si(111)-(1×1) and (3×1) surfaces are shown. The perfect single domain reconstruction existed only over a range of about 4×9 mm^2 in the middle of the sample, due to a temperature gradient on the surface during flashing. Since the light spot was at most 2 mm in diameter this did not affect the photoemission measurements.

The photoemission data in Figs. 2–6 were acquired at a photon energy of $h\nu=34$ eV giving a maximum yield for surface states on Si(111) surfaces.[8] Photon energies in the range of 28 eV$\leqslant h\nu\leqslant$37 eV were used in order to demonstrate that there is no coupling of the observed surface state to bulk states, which would manifest itself by a change of band energies with changing $h\nu$ at fixed parallel momentum $k_\parallel$. The energy resolution was 39 meV for the photons and 33 meV for the electrons with data points every 20 meV. All measurements were performed with p-polarized light with the plane of incidence containing the axis of the electron spectrometer which was fixed at 61° from the incoming photons. The chains in the surface reconstruction were in or perpendicular to this plane. The $E(k)$ band dispersion was mapped by rotating the sample with the rotation axis perpendicular to the plane of incidence while keeping the emission plane equal to it. Angular multidetection covered a range of

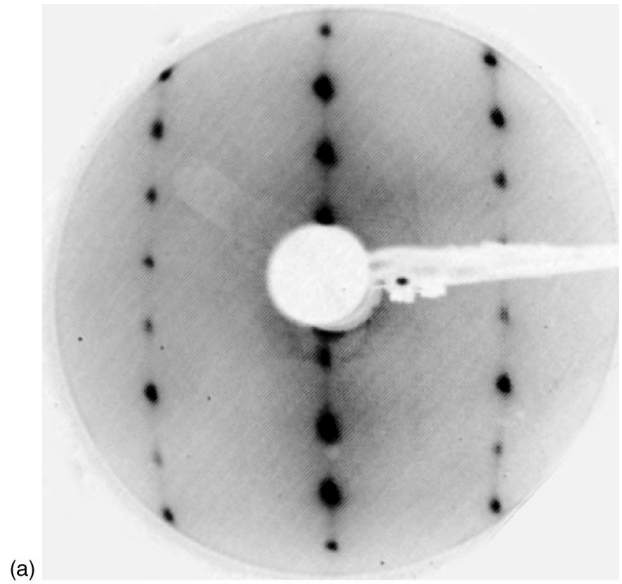

FIG. 1. (a) LEED image of the single-domain Si(111)-(3 $\times$1)-Li surface at 80 eV. (b) Surface Brillouin zones of Si(111)-(1$\times$1) and (3$\times$1) surfaces.

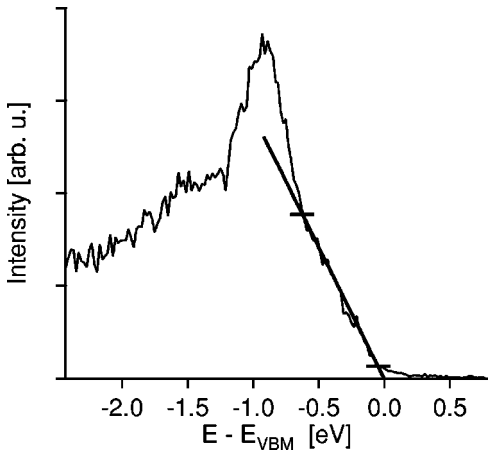

FIG. 2. Energy distribution of photoelectrons from the single-domain Si(111)-(3$\times$1)-Li surface at $k=0$ ($\bar{\Gamma}$). The valence band maximum E_{VBM} is determined from the high-energy cutoff by linear extrapolation.

12° with data points every 0.25°. For optimum overlap of adjacent angular ranges the sample was rotated in steps of 6°. Slight variations of the detector-efficiency times the analyzer transmission as a function of angle were corrected by normalizing the spectra to energy-integrated spectra taken on the secondary electron spectrum. The procedure is to take spectra with identical analyzer settings, just at a photon energy 8 eV higher (42 eV). Energy integrating these spectra yields the detector-efficiency times the analyzer transmission as a function of the emission angle. In panels (a) and (c) in Figs. 3 and 6 these measured angles were converted in values of $k_{\parallel}=\sqrt{(2m/\hbar^2)E_{\mathrm{kin}}}\sin\theta_e$. We used $E_{\mathrm{kin}}=28.5$ eV corresponding to $E-E_{\mathrm{VBM}}=-0.9$ eV where most of the features were observed. In the case of umklapp scattering this procedure leads to an error which is small in the angular range covered and in the case of the (3$\times$1) surface, 0.04 $\mathrm{\AA}^{-1}$ at most. This limit follows from the very value of the reciprocal lattice vector.[45]

As the data were taken while the sample was cooling down a small photovoltage needed to be considered.[40] This effect leads on *n*-type surfaces to a shift of the spectra to lower kinetic energies. Spectra taken at room temperature immediately after the transfer into the analyzer were not yet affected. These were used as energy reference, and the increasing photovoltage shift upon cooling was taken out by adjusting the peak positions in successive spectra with overlapping angular range. Because of the photovoltage there is

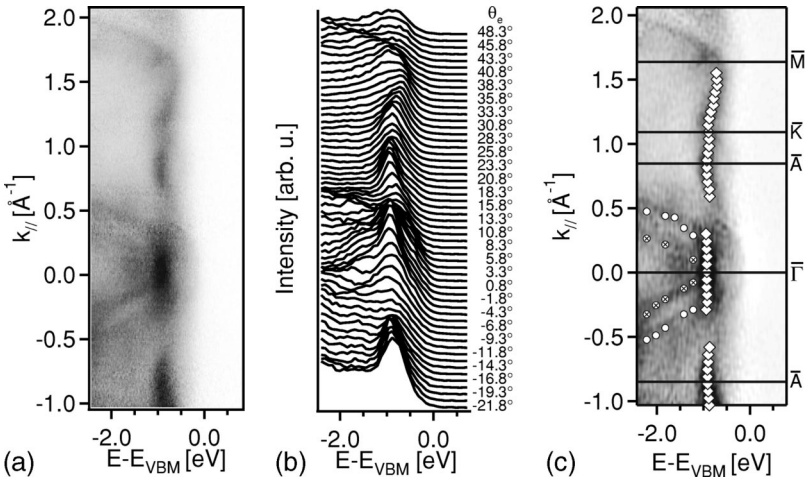

FIG. 3. Photoemission data from the single-domain Si(111)-(3$\times$1)-Li surface for $k_{\parallel}$ along [1$\bar{1}$0], the direction of the chains. (a) Photoemission intensity versus E and $k_{\parallel}$ (high intensity shown dark). (b) Energy distributions versus angle from normal. (c) Data of part (a) after high pass filtering, together with symmetry points of the (3$\times$1) surface [see Fig. 1(b)] and results of peak fits (white diamonds for the surface state and round symbols for the two bulk states).

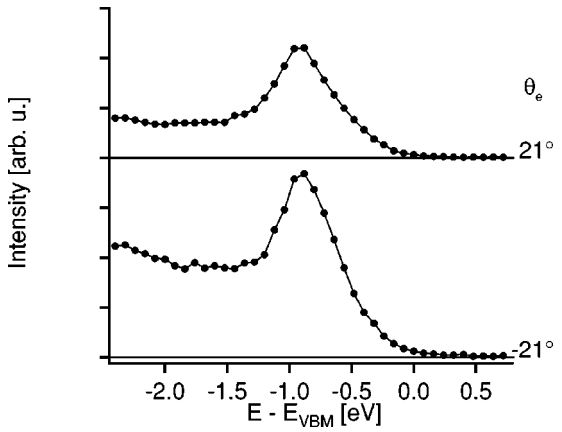

FIG. 4. Energy distribution of photoelectrons from the single-domain Si(111)-(3×1)-Li surface at emission angles of ±21° [see Fig. 3(b)], showing the asymmetry in the intensities at positive and negative emission angles.

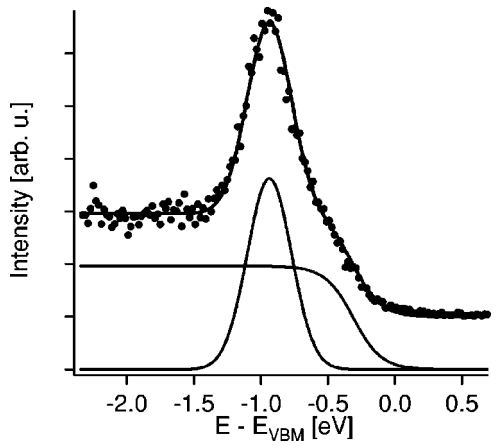

FIG. 5. Energy distribution of photoelectrons from the single-domain Si(111)-(3×1)-Li surface at $\bar{A}$ [see Fig. 1(b)], showing a strong surface state peak for a single-domain sample. A Gaussian fit to the peak position and width plus a fit of a Fermi function to the background is shown.

an uncertainty of about 0.1 eV in the absolute position of the Fermi energy. Therefore, the energy scales in all figures are referred to the valence band maximum (E_{VBM}), which we found to be located at 0.48 eV below the Fermi energy in fair agreement with the value of 0.43 eV from a previous work.[31] This value was obtained by comparing Si $2p$ core level spectra to those of the (7×7) surface where the Fermi level is pinned. E_{VBM} was determined by extrapolating the slope at the high energy end of the spectrum at $\bar{\Gamma}$ to zero yield (Fig. 2). This procedure was independent of the photon energy over the range 22 eV$\leqslant h\nu \leqslant$37 eV (not shown).

Contamination of the surface was monitored by the increase of the oxygen $2p$ peak at -6.2 eV and the decrease of the surface state intensity. A fresh surface was prepared every 30 min.

III. RESULTS

ARPES measurements for electron momenta along the $[1\bar{1}0]$ and $[\bar{1}12]$ crystallographic directions are summarized in Figs. 3 and 6, respectively. Figure 3 gives the $E(k)$ band dispersion along the chains, Fig. 6 perpendicular to them. Panel (b) always shows individual energy distributions at various angles, while panels (a) and (c) represent the photoemission intensity versus E and k (high intensity shown dark). $k_{\|}$ is plotted in the repeated surface Brillouin zone of the (3×1) superlattice. Thereby we automatically take the possibility of surface umklapp scattering [i.e., transfer of reciprocal lattice vectors of the (3×1) surface lattice] into account. Panel (c) has been filtered by a high pass to enhance the visibility of the bands.

The data along the chains in Fig. 3 display a well pronounced surface state band at about 0.9 eV below E_{VBM}. The state exists near the (3×1) Brillouin zone boundary [vertical zig-zag line passing through the $\bar{A}$ point in Fig. 1(b), with $k_{\|}=0.85$ Å^{-1} for $\bar{A}$]. It is quenched near $k_{\|}=\pm 0.5$ Å^{-1} probably due to interaction with the bulk bands (compare Fig. 7). The bulk bands themselves are visible as faint, steeply dispersing parabolas centered around the $\bar{\Gamma}$ point in Fig. 3. They are also visible near the $\bar{M}$ point in the second Brillouin zone at $k_{\|}=1.64$ Å^{-1}, which is equivalent to $\bar{C}$ in the first. There is no intensity at E_F at 0.48 eV above E_{VBM}, confirming that the Si(111)-(3×1)-Li surface is semiconducting. The intensity of the surface state is not

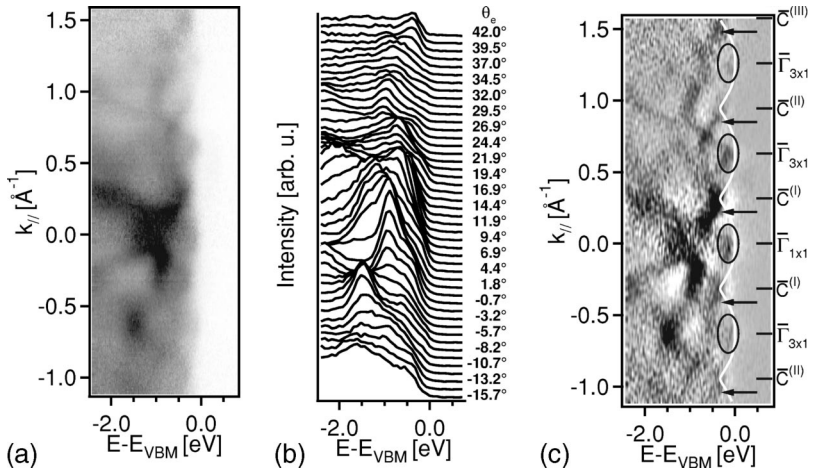

FIG. 6. Photoemission data from the single-domain Si(111)-(3×1)-Li surface for $k_{\|}$ along $[\bar{1}12]$, the direction perpendicular to the chains. (a) Photoemission intensity versus E and $k_{\|}$ (high intensity shown dark). (b) Energy distributions versus angle from normal. (c) Data of part (a) after high pass filtering, together with symmetry points [see Fig. 1(b)] and the top of the projected bulk bands for a (3×1) reconstructed surface (white line, from Ref. 24). The arrows mark a feature that may correspond to a surface state found recently on the Ag induced (3×1) surface (Ref. 24). The ellipses show the periodic appearance of the back folded bulk bands.

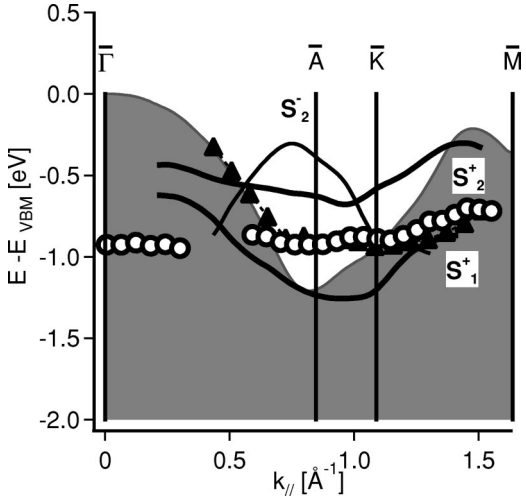

FIG. 7. Band dispersion of surface states on single-domain Si(111)-(3×1)-Li. Open circles are for a single domain (this experiment), full triangles for three domains (from Ref. 31), and lines for a local density calculation of the surface states S_1^+, S_2^+, and S_2^- for the HCC model (Ref. 18). The calculated bands are 0.31 eV higher than the experiments, pointing towards correlation effects on localized states.

symmetric around $\bar{\Gamma}$ in the ARPES spectra. This is seen by comparing the intensities at corresponding positive and negative emission angles, e.g., at $\theta_e = \pm 21°$ (Fig. 4). Such an asymmetry is typical for the photoemission cross section of surface states on Si(111), which tends to be larger for grazing incidence of the light where the perpendicular component of the polarization vector dominates.[8]

Figure 5 shows an individual spectrum of the surface state which demonstrates how pronounced the signal becomes when using a single domain sample. To determine an accurate $E(k)$ dispersion we fitted Gaussians to such energy distributions, as shown in Fig. 5. For the rapidly dispersing bulk bands such fits were performed with the momentum distribution curves (not shown). The positions obtained from such fits are indicated in Fig. 3(c) by white diamonds for the surface state and by round symbols for the two bulk states around $\bar{\Gamma}$. The bulk bands show almost a parabolic dispersion whereas the surface state exhibits only a weak one, which indicates a rather localized state. It is compared with band calculations in Fig. 7.

Figures 6(a)–6(c) show the ARPES data for momenta perpendicular to the chains with k along the $[\bar{1}\bar{1}2]$ ($\bar{\Gamma}$-$\bar{C}$) direction [$\bar{C}$ is the zone boundary of the (3×1) zone perpendicular to the chains at $k_\parallel = 0.315$ Å^{-1}, see Fig. 1(b)]. We suggest that these spectra are dominated by bulk bands originating from the valence band maximum at $k=0$ ($\bar{\Gamma}$). The bulk bands are folded back by the reciprocal lattice vector of the (3×1) reconstruction, which gives some of the features in Fig. 6(c) a periodic appearance [see ellipses and arrows in Fig. 6(c)]. This assignment is corroborated by the white line in Fig.6(c) which marks the top of the projected bulk bands, back folded by the (3×1) surface.[24] Near the minima of the white line one discerns a feature that might be related to a surface state [arrows in Fig. 6(c)]. If true, it would match a recently found state (called S_1) for the Ag-induced single-domain (3×1) surface.[24] In addition a few other features may be visible in Fig. 6(c) (at about −1 eV and below) as well. But as they have no (3×1) periodicity they are related to various superpositions of photoemission spectra from the back-folded bulk bands.

IV. DISCUSSION AND CONCLUSIONS

These photoemission results can be compared to previous photoemission data from three-domain surfaces[31] and to first principles band calculations using the local density approximation (LDA).[18] The band dispersion along the chains agrees between single and multidomain experiments, as shown in Fig. 7 (circles versus triangles). Minor differences exist in k regions where the photoelectron yield from the surface is very weak (around $k_\parallel = 0.7$ Å^{-1}). Both data sets are also consistent in the sense that they show only one surface state at −0.9 eV. The calculations, however, predict two surface state bands with the correct symmetry to be observable, i.e., S_1^+ and S_2^+ (bold lines in Fig. 7). They are separated by 0.6 eV at $\bar{A}$, and the experimental band falls between them. That suggests two possible explanations. Either, the observed band is an unresolved combination of S_1^+ and S_2^+, or the calculated bands need to be shifted down in energy such that the photoemission results correspond more favorable with the data. The necessary shift is 0.31 eV. S_1^+ would end up inside the projected bulk bands in that case and loses mainly its surface character.

We can rule out the first interpretation based on the well-defined, sharp peaks observed for single domain surfaces, such as that shown in Fig. 5 (full width half maximum 0.33 eV). The multidomain data gave less-defined, broader features (full width half maximum 0.7–0.8 eV), which did not allow a distinction. In fact, the interpretation as unresolved peaks was favored in Ref. 31.

To further corroborate the interpretation as down-shifted bands one can search for vestiges of the lower band (S_1^+). It is interesting to note that a feature exists near $\bar{\Gamma}$ in our data with an energy of −0.9 eV (open circles in Fig. 7). It would connect with the calculated S_1^+ band after the downward shift of 0.31 eV required to match the S_2^+ band. A photoemission experiment using Ba as adsorbate[23] found a weak surface state (called S_3), which may correspond to S_1^+ in the nomenclature used here.

The third band in the calculation (S_2^-) has odd parity. As explained in Ref. 18 the plane defined by the $[1\bar{1}0]$ direction and the surface normal is an approximate mirror plane in respect to the Si surface atoms which predominantly generate the surface states (the Li atom turns out to be completely ionized, at least theoretically). If so, the matrix element for photoemission in our geometry (polarization parallel to the approximate symmetry plane) would be very small. And indeed an experiment with a the Ba induced (3×1) reconstruction[23] supports this reasoning. This experiment was performed with both polarization directions and the S_2^- band was found only for the perpendicular light polarization. We were not able to perform a measurement in this geometry

as it was not possible to rotate the experimental chamber.

The energy shift of 0.31 eV required to bring experiment and theory into coincidence may have its origin in the inherent limitations of LDA calculations, particularly when applied to semiconductor surfaces.[41] First of all, the LDA eigenvalues are for a neutral ground state that does not match the positive ion state created in photoemission. The LDA approach becomes particularly questionable for localized states with large electron correlations. Roughly speaking, a localized state will be pulled down in energy by the Coulomb attraction of the hole. The observed surface state on Si(111)-(3×1)-Li falls into that category, based on its weak $E(k)$ dispersion and on its localized charge contours in LDA calculations. They show that the state S_2^+ is localized at one Si surface atom in the HCC model (labeled ''a'' in Ref. 18). A similar situation has been encountered for H-induced surface states on Si(111), where LDA energies come out too high by almost 0.5 to 1 eV relative to E_{VBM}.[42] Quasiparticle calculations of the excited hole state within the GW approximation are able to explain the shift in large part.[42] With these results in mind it is suggestive to assume that the LDA calculations underbind the weakly dispersing states by -0.3 to -0.4 eV. An investigation of these final state effects with methods, such as dynamical mean-field theory of strongly correlated fermion systems[41,43,44] would probably shed new light to this interesting problem.

In conclusion the electronic structure of the single-domain Si(111)-(3×1)-Li surface was studied by means of angular resolved photoemission spectroscopy using single-domain surfaces and improved resolution. The observed surface state originates from a single band, which is shifted down from its LDA energy by 0.31 eV due to final state effects within the localized surface electrons.

ACKNOWLEDGMENTS

This work was supported by the Deutsche Forschungsgemeinschaft (DFG), Bonn, Germany. The authors would also like to thank the staff of the Synchrotron Radiation Center (SRC) where this work was conducted. The SRC is supported by the NSF under Award No. DMR-0084402, FJH by NSF under Award No. DMR-9815416.

*Electronic address: Christian.Bromberger@mpi-hd.mpg.de

[1] F.J. Himpsel, K.N. Altmann, R. Bennewitz, J.N. Crain, A. Kirakosian, J.-L. Lin, and J.L. McChesney, J. Phys.: Condens. Matter **13**, 11 097 (2001).
[2] H.W. Yeom, S. Takeda, E. Rotenberg, I. Matsuda, K. Horikoshi, J. Schaefer, C.M. Lee, S.D. Kevan, T. Ohta, T. Nagao, and S. Hasegawa, Phys. Rev. Lett. **82**, 4898 (1999).
[3] I.R. Collins, J.T. Moran, P.T. Andrews, R. Cosso, J.D. O'Mahony, J.F. McGilp, and G. Margaritondo, Surf. Sci. **325**, 45 (1995).
[4] I.G. Hill and A.B. McLean, Phys. Rev. B **55**, 15 664 (1997).
[5] R. Losio, K.N. Altmann, and F.J. Himpsel, Phys. Rev. Lett. **85**, 808 (2000).
[6] P. Segovia, D. Purdie, M. Hengsberger, and Y. Baer, Nature (London) **402**, 504 (1999).
[7] R. Losio, K.N. Altmann, A. Kirakosian, J.-L. Lin, D.Y. Petrovykh, and F.J. Himpsel, Phys. Rev. Lett. **86**, 4632 (2001).
[8] K.N. Altmann, J.N. Crain, A. Kirakosian, J.-L. Lin, D.Y. Petrovykh, F.J. Himpsel, and R. Losio, Phys. Rev. B **64**, 035406 (2001).
[9] I.K. Robinson, P.A. Bennett, and F.J. Himpsel, Phys. Rev. Lett. **88**, 096104 (2002).
[10] J.N. Crain, K.N. Altmann, C. Bromberger, S.C. Erwin, A. Kirakosian, J.L. McChesney, J.-L. Lin, and F.J. Himpsel, Phys. Rev. Lett. **90**, 176805 (2003).
[11] H. Daimon and S. Ino, Surf. Sci. **164**, 320 (1985).
[12] E. Bauer and H. Poppa, Thin Solid Films **12**, 167 (1972).
[13] H. Kleine, H. Bludau, H. Over, and D. Fick, Surf. Sci. **410**, 15 (1998).
[14] J.J. Paggel, G. Neuhold, H. Haak, and K. Horn, Phys. Rev. B **52**, 5813 (1995).
[15] S. Hasegawa, M. Maruyama, Y. Hirata, D. Abe, and H. Nakashima, Surf. Sci. **405**, L503 (1998).
[16] L. Lottermoser *et al.*, Phys. Rev. Lett. **80**, 3980 (1998).
[17] C. Collazo-Davila, D. Grozea, and L.D. Marks, Phys. Rev. Lett. **80**, 1678 (1998).
[18] S.C. Erwin and H.H. Weitering, Phys. Rev. Lett. **81**, 2296 (1998).
[19] M.-H. Kang, J.-H. Kang, and S. Jeong, Phys. Rev. B **58**, R13 359 (1998).
[20] A.A. Saranin, A.V. Zotov, V.G. Lifshits, M. Katayama, and K. Oura, Surf. Sci. **426**, 298 (1999).
[21] A.A. Saranin, A.V. Zotov, V.G. Lifshits, J.-T. Ryu, O. Kubo, H. Tani, T. Harada, M. Katayama, and K. Oura, Phys. Rev. B **58**, 3545 (1998).
[22] H. Kleine and D. Fick, New J. Phys. **3**, 1.1 (2001).
[23] T. Okuda, H. Ashima, H. Takeda, K.-S. An, A. Harasawa, and T. Kinoshita, Phys. Rev. B **64**, 165312 (2001).
[24] M. Gurnett, J.B. Gustafsson, K.O. Magnusson, S.M. Widstrand, and L.S.O. Johansson, Phys. Rev. B **66**, 161101 (2002).
[25] M. Tikhov, L. Surnev, and M. Kiskinova, Phys. Rev. B **44**, 3222 (1991).
[26] D. Jeon, T. Hashizume, T. Sakurai, and R.F. Willis, Phys. Rev. Lett. **69**, 1419 (1992).
[27] S. Jeong and M.-H. Kang, Phys. Rev. B **54**, 8196 (1996).
[28] C. Bromberger, Ph.D. thesis, Philipps-Universität Marburg, Germany, 2003.
[29] D. Fick, R. Veith, H.D. Ebinger, H.J. Jänsch, C. Weindel, H. Winnefeld, and J.J. Paggel, Phys. Rev. B **60**, 8783 (1999).
[30] H. Winnefeld *et al.*, Phys. Rev. B **65**, 195319 (2002).
[31] H.H. Weitering, X. Shi, and S.C. Erwin, Phys. Rev. B **54**, 10 585 (1996).
[32] R. Losio, K.N. Altmann, and F.J. Himpsel, Phys. Rev. B **61**, 10 845 (2000).
[33] J.N. Crain, K.N. Altmann, C. Bromberger, and F.J. Himpsel, Phys. Rev. B **66**, 205302 (2002).
[34] H.H. Weitering, J. Chen, N.J. DiNardo, and E.W. Plummer, J. Vac. Sci. Technol. A **11**, 2049 (1993).
[35] C. Weindel, H. J. Jänsch, J. J. Paggel, R. Veith, and D. Fick, Surf. Sci. (to be published).
[36] A. Kirakosian, R. Bennewitz, J.N. Crain, T. Fauster, J.-L. Lin, D.Y. Petrovykh, and F.J. Himpsel, Appl. Phys. Lett. **79**, 1608 (2001).
[37] J. Viernow, J.-L. Lin, D.Y. Petrovykh, F.M. Leibsle, F.K. Men,

and F.J. Himpsel, Appl. Phys. Lett. **72**, 948 (1998).
[38] Y.-N. Yang, E.S. Fu, and E.D. Williams, Surf. Sci. **356**, 101 (1996).
[39] S. Olthoff and M.E. Welland, J. Vac. Sci. Technol. B **14**, 1019 (1996).
[40] M. Alonso, R. Cimino, and K. Horn, Phys. Rev. Lett. **64**, 1947 (1990).
[41] W.G. Aulbur, L. Jönsson, and J.W. Wilkins, Solid State Phys., Adv. Res. Appl. **54**, 1 (2000).
[42] X. Blase, X. Zhu, and S. Louie, Phys. Rev. B **49**, 4973 (1994).
[43] G.D. Mahan, *Many-particle Physics*, 3rd ed. (Kluwer Academic/Plenum, New York, 2000).
[44] P. Pou, R. Perez, F. Flores, A.L. Yeyati, A. Martin-Rodero, J.M. Blanco, F.J. Garcia-Vidal, and J. Ortega, Phys. Rev. B **62**, 4309 (2000).
[45] The emission angle of an electron scattered by the umklpapp process would be $\theta_{i+G}=\arcsin[(k_i+G)/\text{const}]$. In our presentation we assumed that this is the same as $\theta_i+\theta_G=\arcsin((k_i/\text{const})\sqrt{1-(G/\text{const})^2}+(G/\text{const})\sqrt{1-(k_i/\text{const})^2})$.